ELECTROMAGNETIC FORCE OF HIGH-SPEED SOLENOID VALVE BASED ON CORRELATION ANALYSIS

Xu De, Fei Hong-Zi, Liu Peng, Zhou Wei and Fan Li-Yun
School of Power and Energy Engineering
Harbin Engineering University, Nantong Street, Nangang District
Harbin City, 150001, China
Emails: xd_heu@163.com, hrbdllp@163.com, fhz@hrbeu.edu.cn, fanly_01@163.com

Submitted: Aug. 14, 2015 ***Accepted: Nov. 4, 2015*** ***Published: Dec. 1, 2015***

Abstract- High-speed solenoid valve (HSV) is the heart of electronic control fuel system for diesel engines, whose electromagnetic force (EF) determines the dynamic response speed of fuel system. The finite element model of HSV has been established and validated by experiment. Methods of experimental design and correlation analysis have been used for the simulation experiment. The effect laws of six key parameters' interactions on EF under HSV's overall operating conditions have been revealed from the results of the simulation. In addition, three key second-order factors' interaction principles are explained. Results show that under overall operating conditions HSV's EF is influenced not only by its parameters singly, but also parameters' interactions.

Index terms*:* High-speed solenoid valve, electronic control fuel system, experimental design, interaction principles.

I. INTRODUCTION

With the increasing concern about the pollutant emission and energy shortage, the requirements of economy and emission for diesel engine become increasingly strict. Then the electronic control fuel system has become the development trend of modern diesel engine's fuel injection system and also the research hotspot [1-5]. The electronic control fuel system mainly includes electronic controlled unit injector system [6], electronic unit pump system [7], high-pressure common rail system [8] and so on. Whereas high-speed solenoid valve (HSV) is one of the most important parts of electronic control fuel system for diesel engine, its dynamic response characteristics have a significant influence on the control precision of fuel injection duration and timing [9-11]. Heightening the dynamic response speed of HSV will improve the control precision of fuel injection duration and timing. As a result, the diesel engine's economy and emission are improved. Thus, it is of great significance to carry out research on HSV.

At present many researches regarding this subject have been carried out, mostly focusing on the modeling and control method of HSV. In [12], a plunger-type solenoid is investigated, by introducing appropriate assumptions, the author developed a set of equations which requires small amount of computer time to execute. These equations describe the de-energizing state of solenoids and perform test results satisfactorily. In [13], an injection quantity simulator was developed to investigate the relation between armature and the injection quantity, and it devised a current waveform control technique to reduce the armature bounce, so the linearity of the injection quantity characteristics is improved. In [14], a novel magnetic levitation system using the eddy current repulsion mechanism is proposed, finite-element approach is used for the analysis of the magnetic field, the structure showed a larger repulsive force comparing to the general electromagnetic, and the precision of the control system can be higher. In [15], a computer program is developed for simulating and predicting the performance of two-valve solenoid actuators, which contains a module for magnetic field analysis and force calculations and a dynamic simulation module which predicts the effects of specific magnetic designs on solenoid opening and closing dynamic performance. In [16], it proposes a feedback control method for a linear resonant actuator (LRA), in which an external load estimated from two signals of the back-EMF is used as a target voltage in PID control. By the estimated load, it becomes possible to obtain an arbitrary amplitude of the mover. In [17], different driving circuits

and control methods of solenoid valve were investigated, and the pre-energizing and reverse-energizing control strategy was applied to speed up the response of solenoid valve.

However, the structure of HSV itself is of importance to speed up the dynamic response speed of HSV, because its performance can be limited by the initial designs such as structure parameters, coil turns and driving current. The strong EF of HSV makes a big influence on its dynamic response speed and the stability of electronic control fuel system, but due to the HSV's operating characteristics and its structure parameters and parameters' interactions, EF has complicated change rules. Therefore, it is important to reveal the effect laws of the key parameters and parameters' interactions on the EF in overall operating conditions, which can provide certain theoretical guidance for HSV's optimization design and is of great importance to create the HSV's prediction mathematic model. At last, the precision of electronic control fuel injection system is improved.

In this paper the finite element model (FEM) of HSV has been developed according to its actual structure, and the accuracy of the model has been verified by experiment. Six key parameters of HSV have been selected, which are pole length, coil turns, coil location, armature thickness, damping hole location and its radius, to try to investigate the effect laws of these parameters' interacting first-order and second-order factors on EF. Then based on HSV's working characteristics its overall operating conditions have been dispersed to nine operating condition points formed by the driving currents and working air gaps. With the experimental design and the method of correlation analysis, correlation coefficients of the first-order and second-order factors with EF of HSV have been gotten under overall operating conditions. By analyzing the correlation coefficients, some important rules of the first-order and second-order factors on EF under overall operating conditions have been revealed. Coil turns and armature thickness have been shown to have significant influence on EF of HSV under overall operating conditions in first-order factors. Moreover interaction principles between coil turns and armature thickness, armature thickness and damping hole location, damping hole location and damping hole radius have been explained in second-order factors' analysis.

The rest of this paper is organized as follows. HSV's structure and working principle in fuel injection system have been described briefly in section II. The methodology and research flow chart of this paper are described in section III. HSV's finite element model and its experimental validation are presented in section IV. Experimental parameters' detailed introduction, operating

points' selection and experimental design are presented and explained in section V. Section VI are the correlation analysis of the 27 factors with EF and the interaction principles between coil turns and armature thickness, armature thickness and damping hole location and damping hole location and damping hole radius. Conclusions are made in section VII.

II. HSV IN FUEL INJECTION SYSTEM

This paper focuses on one kind of HSV of electronic control fuel system. HSV mainly includes armature, iron core, coil, valve stem, reset spring and plug. The materials of armature and iron core are DT4 electrician pure iron and silicon steel sheets respectively, while valve stem, reset spring and plug are made of nonmagnetic materials. So armature and iron core take the main role in creating the EF of HSV， figure 1 has shown the schematic of HSV, and the iron core is made up by main pole and side pole.

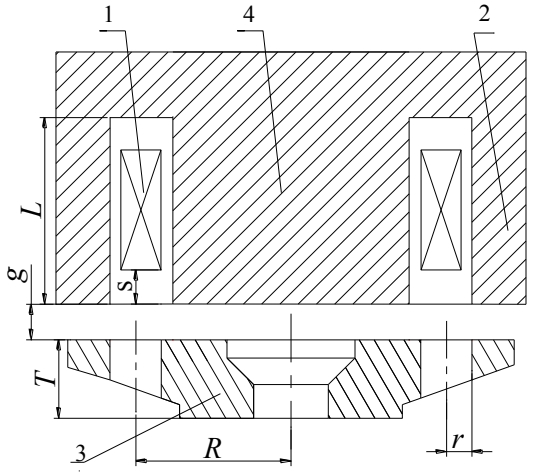

1. Coil 2. Side pole 3. Armature 4. Main pole

Figure 1. Schematic of HSV and its key parameters

When the coil is powered, the magnetic flux is generated in the iron core and armature, so the iron core attracts the armature. When the current of coil is interrupted, the magnetic flux disappears, so the armature is released and reset by spring force. Moreover, the open and closure of fuel injection valve depends on the movement of armature. So the fuel injection can be precisely controlled by the precise control of the movement of armature.

III. METHODOLOGY

The entire process and method of this paper are shown in Figure 2. Firstly, FEM of HSV was developed and validated. Secondly, the operating points were selected according to the working characteristics of HSV to stand for its overall operating conditions. Thirdly, the key parameters of HSV and their each three-level values were determined. Fourthly, by the method of experimental design, the sample points of correlation analysis were obtained. Fifthly, HSV's EF was calculated at every sample point by FEM. Sixthly, the correlation coefficients were computed and gotten based on the method of correlation analysis. Seventhly, by analyzing the correlation coefficients, effect laws of the first-order and second-order factors on EF under overall operating conditions were revealed, based on this, the interaction principles between coil turns and armature thickness, armature thickness and damping hole location, damping hole location and damping hole radius were explained.

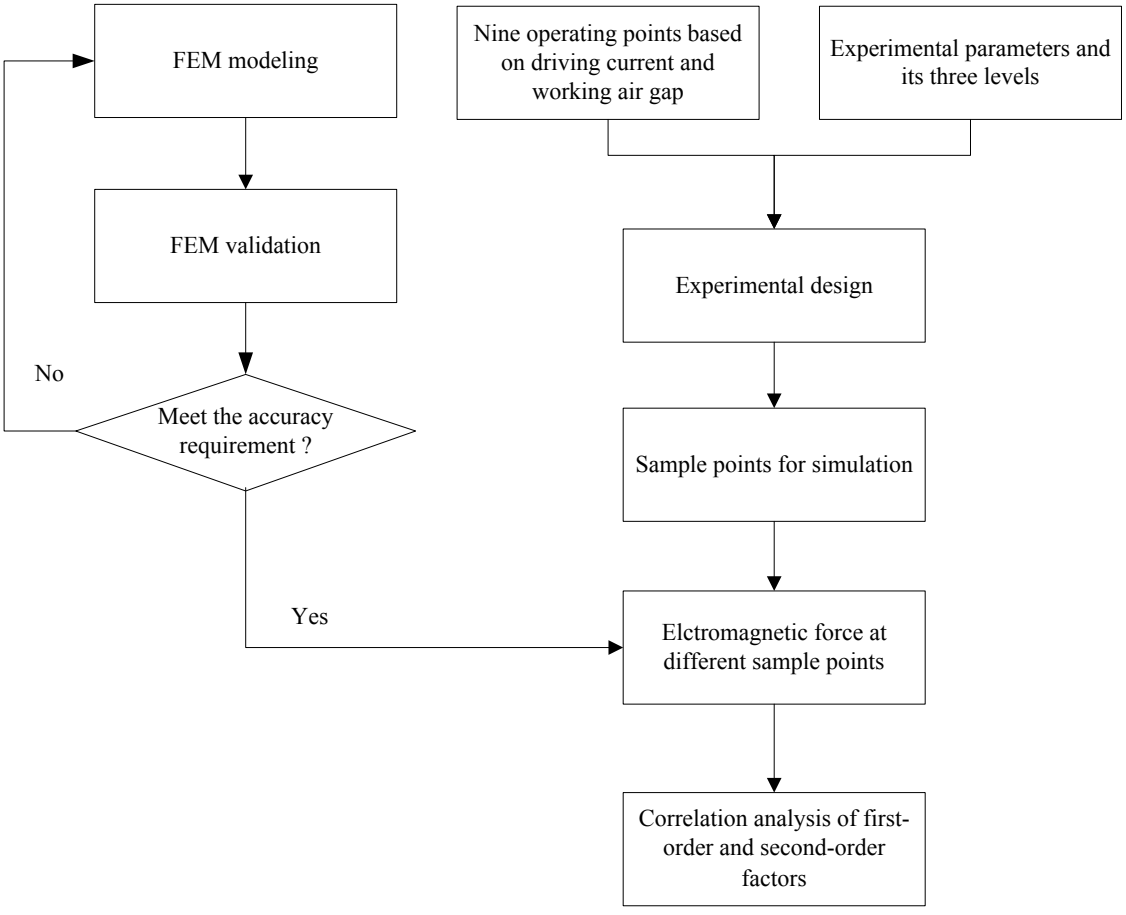

Figure 2. Research flow chart

IV. FEM MODELING AND ITS VALIDATION

a. Computation Model of EF

Maxwell equations for the magnetostatic field are as follow.

$$\begin{cases} \nabla \times H = J \\ \nabla \bullet B = 0 \end{cases} \tag{1}$$

Where H is the magnetic field intensity, J is the current density, B is the magnetic induction intensity.

The EF is computed by the virtual work principle.

$$F_{\text{mag}} = \mathrm{d}W(s,i)/\mathrm{d}s \tag{2}$$

Where F_{mag} is the EF on the armature in the direction of the displacement, $W(s,i)$ is the magnetic co-energy of the system, s is virtual displacement of armature and i is the current of coil. $W(s,i)$ is given by,

$$W(s,i) = \int_V \left(\int_0^H B \cdot \mathrm{d}H \right) \mathrm{d}V \tag{3}$$

Where V is the virtual space surrounding the armature.

After combining equations (2) with (3), we get,

$$F_{\text{mag}} = \frac{\partial}{\partial s} \left[\int_V \left(\int_0^H B \cdot \mathrm{d}H \right) \mathrm{d}V \right] \tag{4}$$

The finite element method is used to solve the equations (1) and get the H and B of entire solution domain. Finally, the EF is computed by the equations (4).

b. Model Validation

The measurement of EF in armature caused by the attraction of iron core is in the electromagnet test-bed. Experimental setup is shown in figure 3. The test-bed mainly includes HSV, bench, S type force sensor, current control drive, current probe, and amplifier. Iron core and S type force sensor are placed at the bench free end and the bench fixed end respectively. And the armature is connected to the S type force sensor between the iron core and the S force sensor. The position of iron core relative to armature can be adjusted freely by the bench free end. When the coil of HSV

is powered, the armature is attracted to the iron core, and then a weak voltage signal is generated by the S type force sensor and amplified by the high precision amplifier. The voltage signal provides the size of EF on armature. The current of coil is adjusted by the current control drive and measured by the current probe.

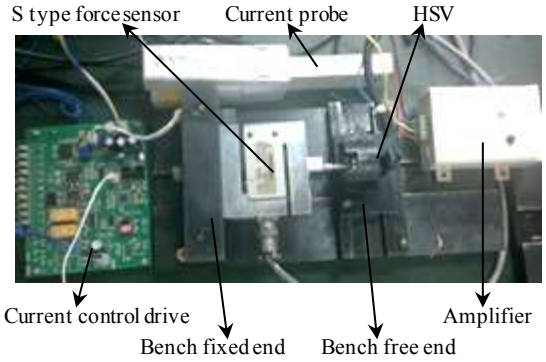

Figure 3. The figure of electromagnet test-bed

Figure 4 shows the changes of FEM results and measurement values along with the change of driving current when the working air gap is 0.2 mm, 0.15 mm, and 0.1 mm respectively. It is easy to infer that the FEM and measurement results match closely under different driving currents and working air gaps and the maximum error is 6%. The error is caused by follows: firstly, the FEM uses initial magnetization curve to approximate magnetization process of soft magnetic materials of HSV; secondly, FEM ignores the heat effect in the HSV' real working condition [18]. As the FEM's accuracy meets the requirement of engineering needs, the FEM can accurately predict the EF of HSV in this paper's analysis.

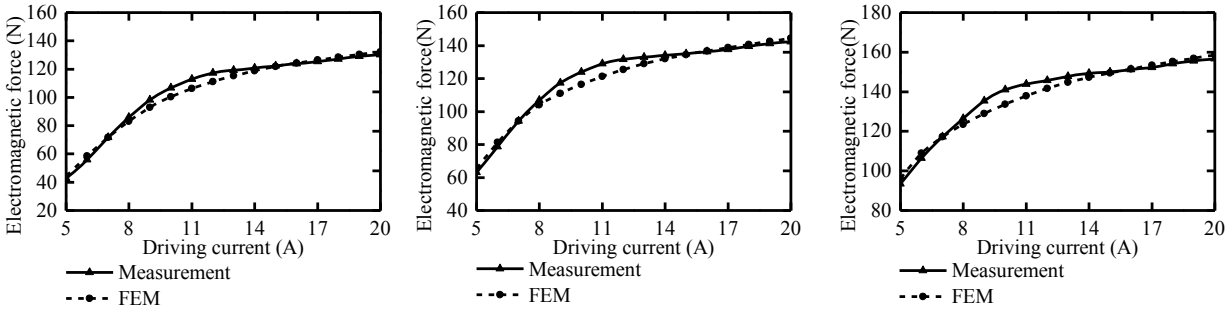

(a) 0.2 mm (b) 0.15 mm (c) 0.1 mm

Figure 4. Comparisons between the FEM and measurement results

V. PARAMETERS AND OPERATING CONDITIONS OF HSV, EXPERIMENTAL DESIGN

Key parameters of HSV selected in this paper mainly include pole length *L*, coil turns *n*, coil location *s* (the distance between coil and working air gap), armature thickness *T*, damping hole location *R* (the distance between damping hole and armature's center) and damping hole radius *r*. The parameters have been shown in figure 1.

Driving current and working air gap are the important parameters affecting the characteristics of HSV. Considering the operating performance of HSV, it uses three levels of current 5 A, 12.5 A, 20 A (small, medium, large) and three levels of working air gap 0.1 mm, 0.15 mm, 0.2 mm (small, medium, large) to stand for HSV's overall operating conditions. As shown in figure 5, the overall operating conditions has been dispersed to nine operating points (5 A，0.1 mm)、(5 A，0.15 mm)、(5 A，0.2 mm)、(12.5 A，0.1 mm)、(12.5 A，0.15 mm)、(12.5 A，0.2 mm)、(20 A，0.1 mm)、(20 A，0.15 mm)、(20 A，0.2 mm) by six characteristic lines. By the research on the EF in these nine operating points, the response characteristics of the HSV's EF in overall operating conditions are obtained.

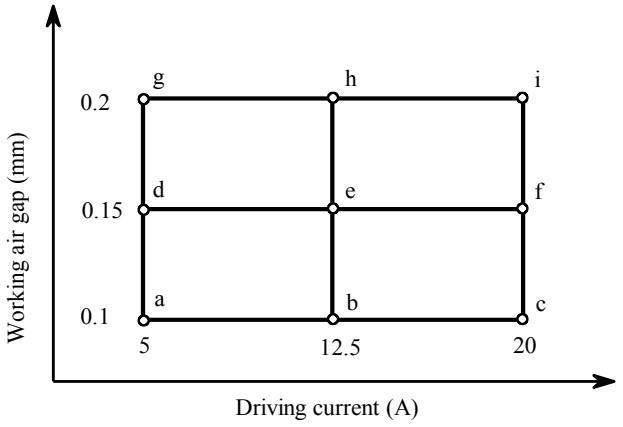

Figure 5. Schematic of overall operating conditions

Central Composite Designs (CCDs) is one of experimental design methods widely used by scientists and technologists. It combines the traditional way of the dispersion of interpolation nodes with the design of full factor and fractional factor, which can provide more information (such as the effect of variable, and test error, etc.) with experiments as little as possible. Classical

CCDs mainly contains these three parts: (1) 2^k factorial designs or fractional factorial designs; (2) $2k$ axial points; (3) a series of central points, where k means the number of the selected parameters [19]. The CCDs has been shown as figure 6 when k is 2, the distance is ± 1 (variables use standardized unit) from the central point (located in the center of the quadrangle) to factors (four vertices of the quadrangle), the distance is $\pm \alpha$ from axial points (located in coordinate axis expect the central point) to central point. By the CCDs, the effective sample points of experiment can be obtained instead of making researches at the whole sample points, which can save much time and work [20]. Then the individual and interactive effects of the key parameters affecting the EF of HSV can be revealed, which provides a full insight of interaction between these key parameters.

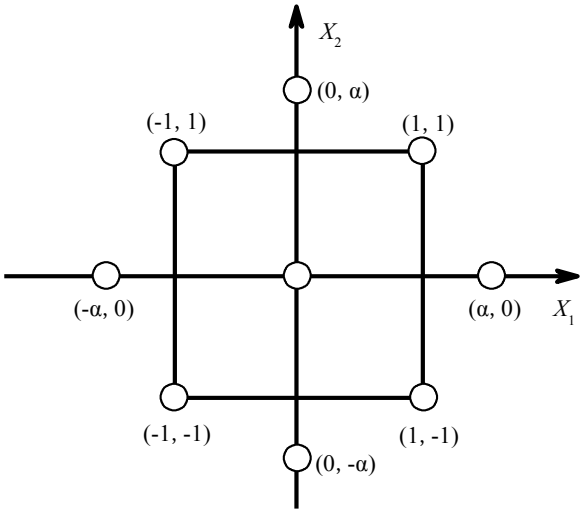

Figure 6. CCDs of two factors

This paper uses the 6 parameters introduced above as the experimental factors (independent variable) of experimental design, which means k is 6, and α is defined as 1. EF is the response variable. Based on the actual value of each of the 6 factors, three-level values of each experimental factor are identified as shown in Table 1, and the 0-level value means the reference value of the factor, -1-level and +1-level values are their each minimum and maximum values. Experimental sample points are obtained based on the combinations of the 6 factors' three-level values. And by CCDs, for nine operating points of the overall operating condition of HSV and three levels of each 6 factors, it only requires 47×9=423 groups of experiments, while in the

condition of full factors $3^6 \times 9 = 9561$ groups of experiments must be conducted to investigate in conventional research method. It can be seen that method of CCDs not only avoids huge amount of workload, but also can guarantee the reliability of the experimental sample points.

Table 1: Three-level values of each experimental factor

Experimental factors	-1-level	0-level	+1-level
Pole length *L*/mm	7	9.5	12
Coil turns *n*/turns	40	60	80
Coil location *s*/mm	0	0.6	1.2
Armature thickness *T*/mm	2.5	4	5.5
Damping hole location *R*/mm	4.2	6.4	8.6
Damping hole radius *r*/mm	0	1	2

VI. CORRELATION ANALYSIS

HSV in electronic control fuel system always works with comprehensive impact of electric field, magnetic field, flow field and mechanical movement [21], the EF is not only influenced by each key parameter separately, but also the interaction between each parameter. And the correlation analysis based on experimental design can not only get the effect laws of single parameter on EF efficiently and accurately, but also can draw more on the effect laws of the parameters' interactions on EF.

Correlation analysis is a method to reveal the mutual relation between two or more parameters. It is not causation and can be quantified by correlation coefficient *R*, whose formula is depicted as equation (5).

$$R = \frac{\sum_{i=1}^{n} (X_i - \bar{x})(y_i - \bar{y})}{\sqrt{\sum_{i=1}^{n} (X_i - \bar{X})^2 \sum_{i=1}^{n} (y_i - \bar{y})^2}} \tag{5}$$

Where *i* is the *i*th sample point, x_i is the value of the *i*th sample point of parameter *x*, $\bar{x}$ is the average value of parameter *x*. As same as parameter *x*, y_i is the value of the *i*th sample point of parameter *y*, $\bar{y}$ is the average value of parameter *y*. Parameter *x* and *y* have a correlation, by the equation (5) value of *R* is computed and gotten between -1 and +1. When *R* is greater than 0, it means *x* and *y* have a positive correlation. When *R* is less than 0, it means *x* and *y* have a negative

correlation. And when R happens to be 0, it means there is no correlation between x and y. Besides, the bigger the absolute value of R is, the more significant the correlation between x and y is.

By CCDs the sample points of every operating condition can be obtained. Then the simulation experiment is carried out by FEM and the simulation results of the sample points are gotten. At last, by the method of the correlation analysis the correlation results of the EF with the 27 factors are found. The 27 factors are formed by the 6 parameters' interactions, which contains 6 first-order factors and 21 second-order factors. The result of correlation analysis has been shown in figure 7, and the X-axis represents the first-order factors and second-order factors formed by the 6 parameters: 1-6 are first-order factors, 1 is pole length L, 2 is coil turns n, 3 is coil location s, 4 is armature thickness T, 5 is damping hole location R, 6 is damping hole radius r. 7-12 are the self-interacting second-order factors, 7 is the second-order factor under the self-interaction of pole length, 8 is the second-order factor under the self-interaction of coil turns, 9 is the second-order factor under the self-interaction of coil location, 10 is the second-order factor under the self-interaction of armature thickness, 11 is the second-order factor under the self-interaction of damping hole location, 12 is the second-order factor under the self-interaction of damping hole radius. 13-27 are second-order factors under the interaction of different parameters, 13 is the second-order factor under the interaction of pole length and coil turns, 14 is the second-order factor under the interaction of pole length and coil location, 15 is the second-order factor under the interaction of pole length and armature thickness, 16 is the second-order factor under the interaction of pole length and damping hole location, 17 is the second-order factor under the interaction of pole length and damping hole radius, 18 is the second-order factor under the interaction of coil turns and coil location, 19 is the second-order factor under the interaction of coil turns and armature thickness, 20 is the second-order factor under the interaction of coil turns and damping hole location, 21 is the second-order factor under the interaction of coil turns and damping hole radius, 22 is the second-order factor under the interaction of coil location and armature thickness, 23 is the second-order factor under the interaction of coil location and damping hole location, 24 is the second-order factor under the interaction of coil location and damping hole radius, 25 is the second-order factor under the interaction of armature thickness and damping hole location, 26 is the second-order factor under the interaction of armature thickness and damping hole radius, 27 is the second-order factor under the interaction of damping hole

location and damping hole radius. The Y-axis represents the factors' corresponding correlation coefficient. It can be seen from figure 7(a), 7(b), 7(c) that how correlation coefficients change with the change of working air gap at different currents, and it can be seen from figure 7(d), 7(e), 7(f) that how correlation coefficients change with the change of current at different working air gaps.

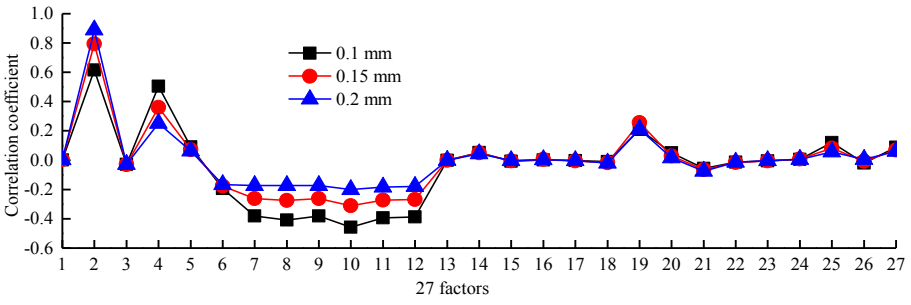

(a) Driving current 5 A

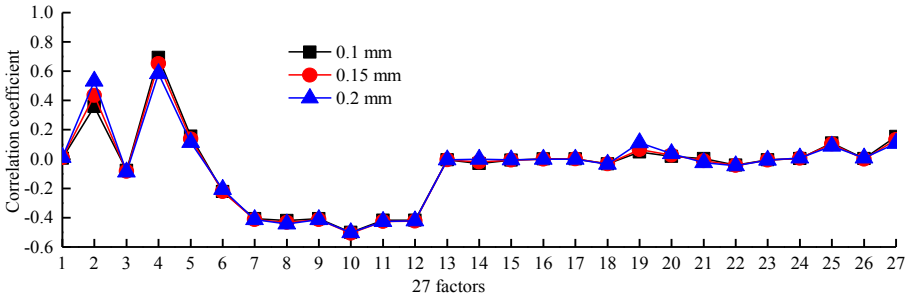

(b) Driving current 12.5 A

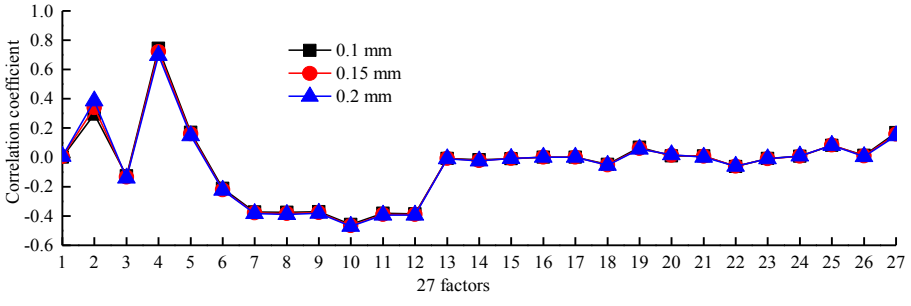

(c) Driving current 20 A

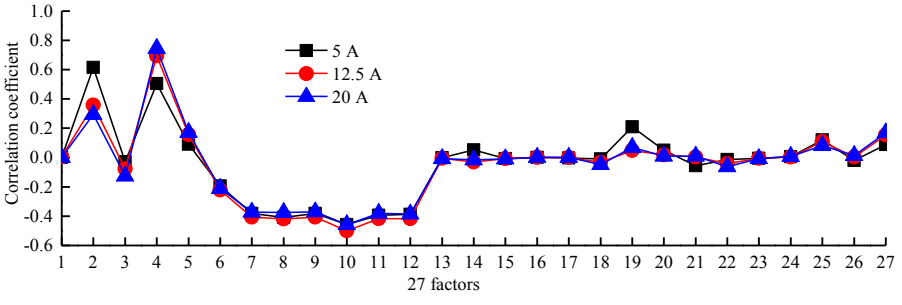

(d) Working air gap 0.1 mm

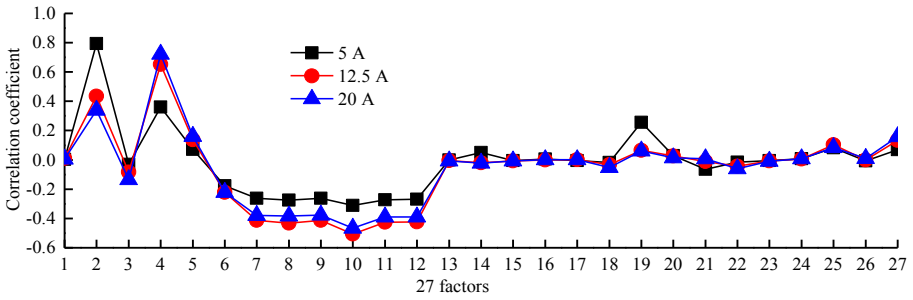

(e) Working air gap 0.15 mm

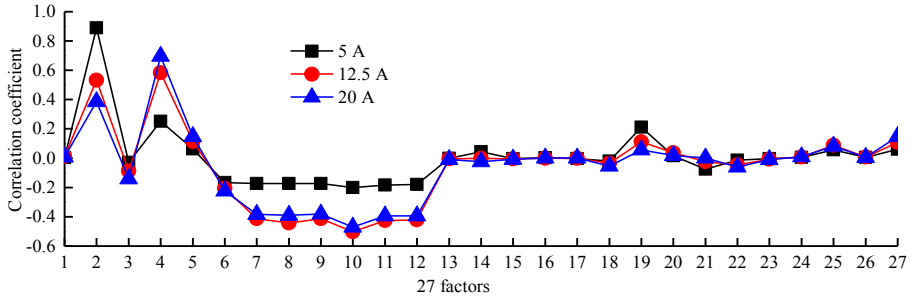

(f) Working air gap 0.2 mm

Figure 7. The correlation coefficients of the 27 factors with EF under overall operating conditions

a. Correlation analysis of first-order factors

The first factor in figure 7 is pole length *L*, the corresponding correlation coefficients are all unobvious at every operating condition. The second factor in figure 7 is coil turns *n*, the corresponding correlation coefficients are all greater than 0 at every operating condition, moreover the absolute value of correlation coefficient decreases with the increase of driving current, and it increases with the increase of working air gap. The third factor in figure 7 is coil location *s*, the corresponding correlation coefficients are all less than 0 at every operating condition, moreover the absolute value of correlation coefficient rises slightly with the increase of driving current, and it mainly keeps the same with the increase of working air gap. The fourth factor in figure 7 is armature thickness *T*, the corresponding correlation coefficients are all greater than 0 at every operating condition, and moreover the absolute value of correlation coefficient increases with the increase of driving current while decreases with the increase of working air gap. The fifth factor in figure 7 is damping hole location *R*, the corresponding correlation coefficients are all greater than 0 at every operating condition, moreover the absolute value of correlation coefficient increases with the increase of driving current while decreases with the increase of working air gap. The sixth factor in figure 7 is damping hole radius *r*, the corresponding correlation coefficients are all less than 0 at every operating condition, moreover the absolute value of correlation coefficient almost keeps the same with the change of the

operating condition.

All of above are the correlation analyses of first-order factors formed by the 6 parameters with EF under overall operating conditions, which reveals the effect laws of each first-order factor on EF with the change of operating condition. It can be seen that coil turns n and armature thickness T have significant influence on EF.

b. Correlation analysis of second-order factors

Factors from the seventh to twelfth in figure 7 are second-order factors formed by the self-interaction of the 6 parameters. Their correlation coefficients are all less than 0 at different operating conditions, and the absolute values of correlation coefficients are all large. When driving current is at a small level, their absolute values of correlation coefficients decrease with the increase of working air gap; yet when driving current is at a high level, their absolute values of correlation coefficients at different working air gaps are all large. The correlation between each of factor 7, 8, 10, 11 and EF is opposite to their each first-order factor's. For second-order factor 7 and 11 the absolute values of correlation coefficients are larger than their each first-order factor's at different operating conditions, which means each influence of the two factors on EF is more significant than their each first-order factor's. So it can be seen that first-order and second-order factors have different effect laws.

The rest factors from the thirteenth to twenty-seventh in figure 7 are second-order factors formed by the different parameters' interactions. Among them the correlation coefficients of factor 19, 25 and 27 are all greater than 0 at each operating condition and their absolute values are all large. The correlation coefficients of factor 18, 21 and 22 are all less than 0 at each operating condition and their absolute values are all large too. Besides, the correlation coefficients of factor 14, 21 and 26 have complicate change rules. So it can be seen that their relations with EF of HSV are complicate and nonlinear.

All of above are the correlation analyses of the 21 second-order factors with EF under overall operating conditions. Among the second-order factors, correlation coefficients of 19, 25, 27 are relatively large, they are respectively the interactions of coil turns and armature thickness, armature thickness and damping hole location, damping hole location and damping hole radius. Then the analysis will be focused on interaction mechanisms of these three factors on EF. The figures of interaction analysis have been shown in figure 8, 9 and 10.

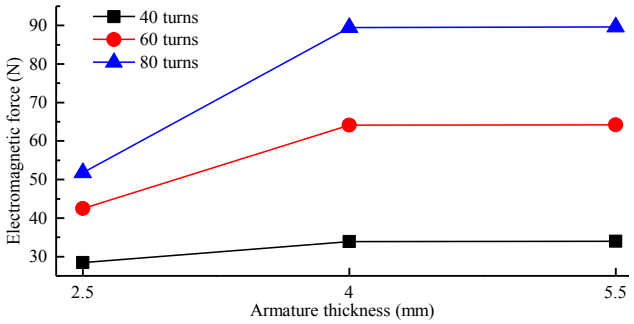

Figure 8. Coil turns and armature thickness

Figure 8 has shown the change of EF of HSV along with the change of armature thickness T at different levels of coil turns and the operating condition (5 A，0.15 mm). From the figure, it can be concluded that the more the coil turns is, the larger the increase of EF with the increase of armature thickness is. It means the influence of armature thickness to EF gets larger when coil turns is at a higher level. It can be explained as follows. Because the more the coil turns is, the stronger the total magnetic motive force of the magnetic circuit of HSV is, so magnetic field in the armature tends to be more saturated. While the increase of armature thickness makes the increase of the flow area of magnetic flux in armature, and at a higher level of coil turns the effect of weakening saturation in armature is more significant. As a result, armature thickness's influence on EF increases. Besides, it also can be seen from the figure that when armature thickness increases from 4 mm to 5.5 mm, EF increases slowly. It is because that the effective flow area of magnetic flux in armature mainly has no change any more when armature thickness increases to a certain value. It has insignificant influence on magnetic field and magnetic flux in armature, then EF increases slowly.

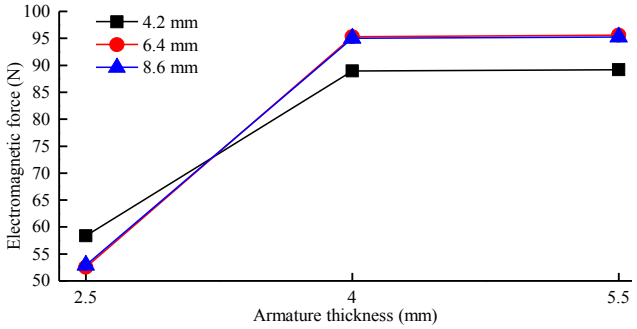

Figure 9. Armature thickness and damping hole location

Figure 9 has shown the change of EF of HSV along with the change of armature thickness T at different levels of damping hole location R and the operating condition (5 A, 0.1 mm). From the figure, it can be concluded that when damping hole location R increases from 4.2 mm to 6.4 mm, the increase of EF with the increase of armature thickness gets larger; while when damping hole location R increases from 6.4 mm to 8.6 mm, the increase of EF with the increase of armature thickness is unobvious. That is when damping hole location is at a higher level, the influence of armature thickness on EF is larger, while when damping hole location's level is too high, the increase of EF with the increase of armature thickness almost keeps the same. The reasons for the phenomenon are the following.

Magnetic flux in armature flows through its radial direction, magnetic line of force gets sparser from the center of the armature to its all around. Therefore, when damping hole location is at a higher level, the influence of damping hole on magnetic line of force decreases. Yet at the same time, armature thickness increases, the sectional area in its radial direction increases, the saturation in armature gets weakened, then magnetic field increases, which in turn makes the influence of armature thickness on EF increases. Therefore, when damping hole location R increases from 4.2 mm to 6.4 mm, the increase of EF with the increase of armature thickness gets larger. But when damping hole location R increases from 6.4 mm to 8.6 mm the sectional area in armature's radial direction of magnetic flux becomes large enough, with the combined action of magnetic resistance and flow area of magnetic flux EF turns out to increase slowly.

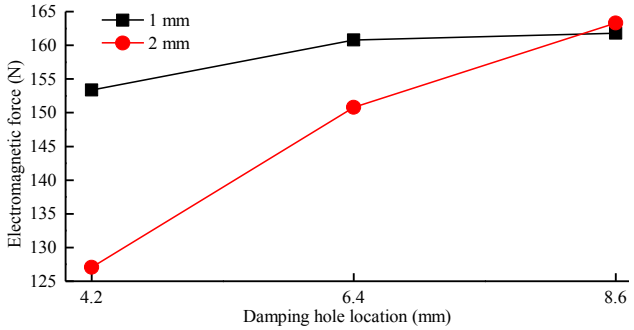

Figure 10. Damping hole location and damping hole radius

Figure 10 has shown the change of EF of HSV along with the change of damping hole location R at different levels of damping hole radius r and the operating condition (20 A，0.1 mm). From the figure, it can be concluded that the larger the damping hole radius is, the larger the increase of EF

with the increase of damping hole location is. That is when damping hole radius is at a higher level, the influence of damping hole location on EF gets larger. The reasons for the phenomenon are the following. The increase of damping hole radius can decrease the flow area of magnetic flux in the armature's radial direction, then magnetic flux tends to be saturated. However, as magnetic line of force gets sparser from the center of the armature to its all around, the saturation gets weakened with the increase of damping hole location. Therefore, the phenomenon introduced above appears. Besides, it also can be seen from the figure that when damping hole location increases from 6.4 mm to 8.6 mm, EF increases slowly. It is because that when damping hole location increases to a certain value, it almost has no influence on the distribution of the magnetic line of force in armature. Therefore, the EF increases slowly.

VII. CONCLUSIONS

The finite element model of HSV was developed according to its real size, and validated by experiment. It reveals the certain effect laws of each first-order factor on EF under overall operating conditions by correlation analysis. The significant first-order factors are coil turns and armature thickness. The correlation of coil turns with the EF decreases with the increase of driving current, while increases with the increase of working air gap. The correlation of armature thickness with the EF increases with the increase of driving current, while decreases with the increase of working air gap.

The correlation between the EF and each self-interacting second-order factor has different effect laws to that of the corresponding first-order factor.

By analyzing the interactions of HSV's different parameters, it reveals: the more the coil turns is, the larger the increase of the EF with the increase of armature thickness is; when damping hole location is at a higher level, the influence of armature thickness on EF is larger, while when damping hole location's level is too high, the increase of EF with the increase of armature thickness almost keeps the same; when damping hole radius is at a higher level, the influence of damping hole location on EF gets larger, while when damping hole radius's level is too high, EF increases slowly. HSV's characteristic of EF is determined by the combined action of its key parameters' interactions.

VIII. ACKNOWLEDGEMENT

This work is supported by the National Natural Science Foundation of China (NSFC 51379041, 51279037, 51475100) and the Key Project of Chinese Ministry of Education (113060A).

REFERENCES

[1] N. Guerrassi and P. Dupraz, "A Common Rail Injection System For High Speed Direct Injection Diesel Engines", SAE Technical Paper 980803, 1998.

[2] K. C. Bayindir, M. A. Gözüküçük and A. Teke, "A comprehensive overview of hybrid electric vehicle: Powertrain configurations, powertrain control techniques and electronic control units", Energy Conversion and Management, vol. 52, No. 2, 2011, pp. 1305-1313.

[3] Q. Hayat, L. Y. Fan, X. Z. Ma and B. Q. Tian, "Comparative Study of Pressure Wave Mathematical Models for HP Fuel Pipeline of CEUP at Various Operating Conditions", International Journal of Smart Sensing and Intelligent Systems, vol. 6, No. 3, 2013, pp. 1077-1101.

[4] L. Y. Fan, P. H. Li and E. Z. Song, "Research on Electronic Control Unit of Electronic Unit Pump Fuel Injection System for Diesel Engines", Proceedings of the 2012 Third International Conference on Mechanic Automation and Control Engineering. IEEE Computer Society, 2012, pp. 605-608.

[5] S. Y. Yang and S. H. Chung, "An experimental Study on the Effects of High-Pressure and Multiple Injection Strategies on DI Diesel Engine Emissions", SAE Technical Paper 2013-01-0045, 2013.

[6] P. Lauvin, A. Löffler, A. Schmitt and W. Zimmermann, "Electronically Controlled High Pressure Unit Injector System for Diesel Engines", SAE Technical Paper 911819, 1991.

[7] C. L. Zhao, "Research on Injection System of Electronic Unit Pump Diesel", Chinese Internal Combustion Engine Engineering, 2004, 2, pp. 22-23.

[8] W. Boehner and K. Hummel, "Common Rail Injection System for Commercial Diesel Vehicles", SAE Technical Paper 970345, 1997.

[9] G. L. Shi, "On the researches of high speed solenoid on/off valve and its applications", Machine Tool & Hydraulics, 2001, 1, pp. 1-2.

[10] L. C. Passarini and P. R. Nakajima, "Development of a high-speed solenoid valve: an investigation of the importance of the armature mass on the dynamic response", Journal of the Brazilian Society of Mechanical Sciences and Engineering, vol. 25, No. 4, 2003, pp. 329-335.

[11] G. Bianchi, P. Pelloni, F. Filicori and G. Vannini, "Optimization of the Solenoid Valve Behavior in Common-Rail Injection Systems", SAE Technical Paper 2000-01-2042, 2000.

[12] Kajima and Takashi. "Dynamic model of the plunger type solenoids at deenergizing state", IEEE Transactions on magnetics, vol. 31, No. 3, 1995, pp. 2315-2323.

[13] R. Kusakabe, M. Abe, H. Ehara and T. Ishikawa, "Injection Quantity Range Enhancement by Using Current Waveform Control Technique for DI Gasoline Injector", SAE Technical Paper 2014-01-1211, 2014.

[14] T. Nakao, H. Han and Y. Koshimoto, "Fundamental study of magnetically levitated contact-free micro-bearing for MEMS applications", International Journal on Smart Sensing and Intelligent Systems, vol. 3, No. 3, 2010, pp. 536-549.

[15] S. Wang, T. Miyano and M. Hubbard, "Personal Computer Design Software for Magnetic Analysis and Dynamic Simulation of a Two-Valve Solenoid Actuator", SAE Technical Paper 921086, 1992.

[16] Asai, Yasuyoshi, K. Hirata, and T. Ota. "Amplitude Control Method of Linear Resonant Actuator by Load Estimation From the Back-EMF", IEEE transactions on magnetics, vol.49, No.5, 2013, pp. 2253-2256.

[17] H. Lu, J. Deng, Z. Hu and Z. Wu, "Impact of Control Methods on Dynamic Characteristic of High Speed Solenoid Injectors", SAE Technical Paper 2014-01-1445, 2014.

[18] S. Domanski, "Effects Contributing to the Temperature Rise of Electromagnetic Actuators", SAE Technical Paper 2000-01-0543, 2000.

[19] Araujo, W. Pedro and Richard G. Brereton, "Experimental design II. Optimization", TrAC Trends in Analytical Chemistry, vol.15, No. 2, 1996, pp. 63-70.

[20] J. D. Tew, "Using central composite designs in simulation experiments", Proceedings of the 24th conference on Winter simulation, 1992, pp. 529-538.

[21] B. Huber and H. Ulbrich, "Modeling and experimental validation of the solenoid valve of a common rail diesel injector", SAE Technical Paper 2014-01-0195, 2014.